A New Relative Receiver Autonomous Integrity Monitoring Algorithm for Multiple Failures

Ho Yun, Deokhwa Han, Hongki Song, Sungyong Lee, and Changdon Kee

Mechanical and Aerospace Engineering and the Institute of Advanced Aerospace Technology, Seoul National University

Abstract

In near future, GNSS GPS modernization, renewed GLONASS and a new Galileo signal will be available. And the accuracy of position solution will be better by courtesy of improved quality of ranging signal. As an expected accuracy is better, the threshold for failure will be reduced. As a result, the prior probability of failures could be larger than what is used now. Due to the increased prior probability of failures, probability of simultaneous multiple failures cannot be neglected any more. Furthermore there will be many more ranging sources makes it necessary to consider the possibility of simultaneous multiple failures. This paper develops and analyzes a new Relative Receiver Autonomous Integrity Monitoring (RRAIM) algorithm which can treat no only a single failure but also simultaneous multiple failures. A proposed algorithm uses measurement residuals and satellite observation matrices of several consecutive epochs for Failure Detection and Exclusion (FDE). It detects failures by monitoring the error vector itself instead of monitoring the projection of the error vector. The simulation results show that the algorithm is able to detect any instance of multiple failures which are not detected by the conventional RAIM algorithm.

Keywords: Multiple failures, FDE, Integrity monitoring, RRAIM

1 Introduction

The advent of new GNSSs such as Galileo, renewed GLONASS, and COMPASS will lead to improved navigation performance. Accuracy will be improved, and the threshold for failure detection will be reduced. As a result, the prior probability of failure under its current definition can be expanded according to the new criteria. Furthermore, due to an increased number of ranging sources, it is necessary to consider the possibility of simultaneous multiple failures.

The Conventional Weighted Least Squares (WLS) FDE algorithm uses a range residual vector to determine whether the current range measurement is normal or not (Walter and Enge, 1995). However, because the range residual is a projection of the range error, it contains only partial information regarding the error. Therefore, the test statistic cannot be used as an absolute indication of satellite failure, and this algorithm cannot be applied in the most general cases. It can only be applied in the case of a single satellite failure. This paper proposes a new RAIM algorithm, which can handle simultaneous multiple failures as well as a single failure. The proposed algorithm uses range residuals and satellite observation matrices of several consecutive epochs for FDE. This concept of FDE was originally proposed by (Martini et al, 2006). It provides a test statistic for comparison with a threshold analogous to the conventional WLS algorithm, but is able to detect all kinds of failures. However, because the magnitude of the Minimum Detectable Bias (MDB) is on the order of 5km with a detection latency of 2 to 5 seconds, it is hard to implement in Safety of Life (SOL) applications. In order to achieve MDBs acceptable for practical applications, the proposed algorithm adopts the Relative RAIM (RRAIM) scheme. In addition, the proposed algorithm combines the backward time difference residual vectors and observation matrices, and it directly estimates the error vector in order to detect failure(s) in range measurement with no latency. The paper begins with an analysis of the characteristics and limitations of the conventional WLS RAIM algorithm, followed by a detailed explanation of a new multiple-hypothesis FDE algorithm with rigorous mathematical expression. Finally, the simulation results are presented to assess performance of the algorithm.

2 Characteristics and limitation of the conventional RAIM algorithm

The conventional WLS FDE algorithm estimates the ranging error via the least square fit and the basic linearized measurement equation.

$$\mathbf{z}_k = \mathbf{H}_k \cdot \mathbf{x}_k + \mathbf{v}_k \tag{1}$$

$$\mathbf{r}_k = \left[\mathbf{I}_k - \mathbf{P}_k\right] \cdot \mathbf{z}_k = \left[\mathbf{I}_k - \mathbf{P}_k\right] \cdot \mathbf{v}_k \tag{2}$$

where $\mathbf{z}_k$ is an N -dimensional vector containing the pseudo-range measurements minus the expected ranging values based on the location of the satellites and the location of the user($\mathbf{x}_k$), $\mathbf{H}_k$ is the observation matrix, and $\mathbf{v}_k$ is

an N -dimensional vector containing the errors in $\mathbf{z}_k$. $\mathbf{I}_k$ is an $\mathbf{N}$ -dimensional identity matrix, $\mathbf{r}_k$ is the range residual vector, and $\mathbf{P}_k$ is defined as

$$\mathbf{P}_k \triangleq \mathbf{H}_k \cdot \mathbf{K}_k \triangleq \mathbf{H}_k \cdot \left[\mathbf{H}_k{}^T \mathbf{R}_k{}^{-1} \mathbf{H}_k\right]^{-1} \mathbf{H}_k{}^T \mathbf{R}_k{}^{-1} \tag{3}$$

where $\mathbf{R}_k = Cov\left[\mathbf{v}_k\right]$. The range residual vector in Eq. (2) can also be expressed as a difference between the measured range and the estimated range, which is calculated from the user's position and clock solution.

$$\mathbf{r}_k = \mathbf{z}_k - \mathbf{H}_k \hat{\mathbf{x}}_k \tag{4}$$

where $\hat{\mathbf{x}}_k = \left[\mathbf{H}_k{}^T \mathbf{R}_k{}^{-1} \mathbf{H}_k\right]^{-1} \mathbf{H}_k{}^T \mathbf{R}_k{}^{-1} \cdot \mathbf{z}_k$.

From the range residual vector, the Weighted Sum of the Squared Errors (WSSE) is defined as a test statistic of FDE.

$$WSSE = \mathbf{r}_k{}^T \cdot \mathbf{R}_k{}^{-1} \cdot \mathbf{r}_k \tag{5}$$

Eq. (2) means that the N -dimensional error vector $\mathbf{v}_k$ is projected onto the null space of $\mathbf{H}_k{}^T$, which has a dimension of N - 4. Like all other projections in subspaces, some information is lost during this transformation, and $WSSE$ contains only partial information. Thus, the test statistic cannot be used as an absolute indication of the quality of $\mathbf{z}_k$ (i.e. the magnitude of $\mathbf{v}_k$).

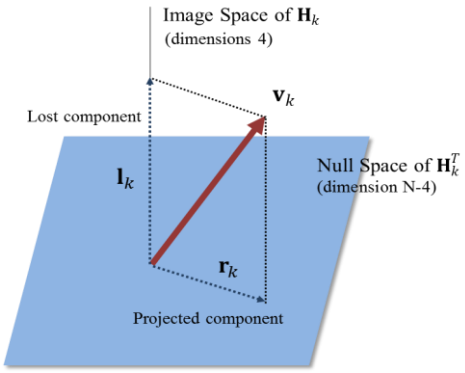

Fig. 1. Lost component of the WLS algorithm

In cases involving multiple failures, position error can grow too large without a corresponding growth in the test statistic (Macabiau et al, 2005). In this case, the conventional RAIM algorithm cannot detect the occurrence of anomalous situations and fails to protect the position solution, risking its integrity. It can be concluded that the conventional WLS algorithm protects the user only in the case of a single failure.

3 New RAIM algorithm considering multiple simultaneous failures

To overcome the limitations of the WLS algorithm, (Martini et al, 2006) introduced a new idea for an FDE algorithm that reconstructs its lost component. Fig. 2 depicts the basic idea of the new FDE technique in a 2D case.

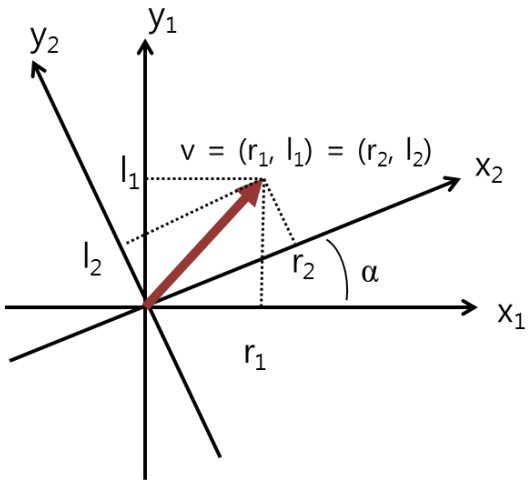

Fig. 2. The FDE technique of Martini et al. (2D case)

This technique can, for example, be used to find the error vector $\mathbf{v}$. In this problem, $\mathbf{r}$ is available at each epoch, but $\mathbf{l}$ is not. The residual vector at each epoch is equivalent to $\mathbf{r}_1$ and $\mathbf{r}_2$, and the lost components are equivalent to $\mathbf{l}_1$ and $\mathbf{l}_2$. The single measurement of $\mathbf{r}_1$ is not sufficient to estimate the vector $\mathbf{v}$, because $\mathbf{r}_1$ has only one degree of information while $\mathbf{v}$ requires two degrees of information. Therefore, two independent observations are necessary to estimate the magnitude of $\mathbf{v}$. $\mathbf{v}$ can be estimated by collecting information from two consecu-

tives epochs and measuring the change in coordinate frame α. This problem can be expressed in terms of the following mathematical expression:

$$\mathbf{v} = (\mathbf{r}_1, \mathbf{l}_1) = (\mathbf{r}_2, \mathbf{l}_2) \tag{6-1}$$

$$\begin{cases} \mathbf{r}_2 = \mathbf{r}_1 \cdot \cos\alpha + \mathbf{l}_1 \cdot \sin\alpha \\ \mathbf{l}_2 = -\mathbf{r}_1 \cdot \sin\alpha + \mathbf{l}_1 \cdot \cos\alpha \end{cases} \tag{6-2}$$

where the unknowns are $\mathbf{v}$, $\mathbf{l}_1$, and $\mathbf{l}_2$, and the observables are $\mathbf{r}_1$, $\mathbf{r}_2$, and α. The next step is to reconstruct the vector $(\mathbf{r}_1, \mathbf{l}_1)$ with known $\mathbf{r}_1$, $\mathbf{r}_2$, and α values. Assuming that $\mathbf{v}$ is constant for two consecutive epochs, $\mathbf{l}_1$ can be calculated as follows:

$$\mathbf{l}_1 = -\frac{\cos\alpha}{\sin\alpha} \cdot \mathbf{r}_1 + \frac{1}{\sin\alpha} \cdot \mathbf{r}_2 \tag{7}$$

In this problem, the two reference systems (x_1Oy_1 and x_2Oy_2) must be linearly independent (i.e. $\alpha \neq 0$).

Expanding this 2D problem to a navigation case, the unknown vector $\mathbf{v}$ has a dimension of N and consists of a bias component and a noise component. The residual vector—the error vector's projection on the null space of H^T (a subspace with a dimension of $N-4$)—is observable. By using the residual vectors of consecutive epochs and taking advantage of the geometric diversity of the constellation, multiple failures can be detected without limitation on the number of components affected by bias in $\mathbf{v}$. Furthermore, it can not only monitor the norm of the residuals vector but also reconstruct the lost component of $\mathbf{v}$. However, the system is ill-conditioned, and the constellation geometry changes slightly over the significant distance between the user and the satellites. Therefore, the algorithm is very sensitive to the magnitude of the error vector. Due to this issue, the MDB with GNSS live signals developed by previous research has been limited to about 5km in magnitude, which prevents the results from being applied to SOL services. Furthermore, it has a detection latency of 2-5 seconds, depending on the number of satellites. This latency may result in a failure to meet the 6-second Time To Alert (TTA) requirement.

This paper proposes a new approach, which can provide an acceptable MDB magnitude with no latency. The proposed algorithm combines the backward time

difference residual vectors and observation matrices, and it directly estimates the error vector $\mathbf{v}_k$ so that it can detect the failure(s) of range measurements with no latency. As shown in Fig. 3 and by Eqs. (2) and (3), the error vector $\mathbf{v}_k$ can be expressed as a sum of the projected component and the lost component.

$$\mathbf{v}_k = \mathbf{r}_k + \mathbf{l}_k = \left(\mathbf{I}_k - \mathbf{H}_k\mathbf{K}_k\right)\mathbf{v}_k + \mathbf{H}_k\mathbf{K}_k\mathbf{v}_k \tag{8}$$

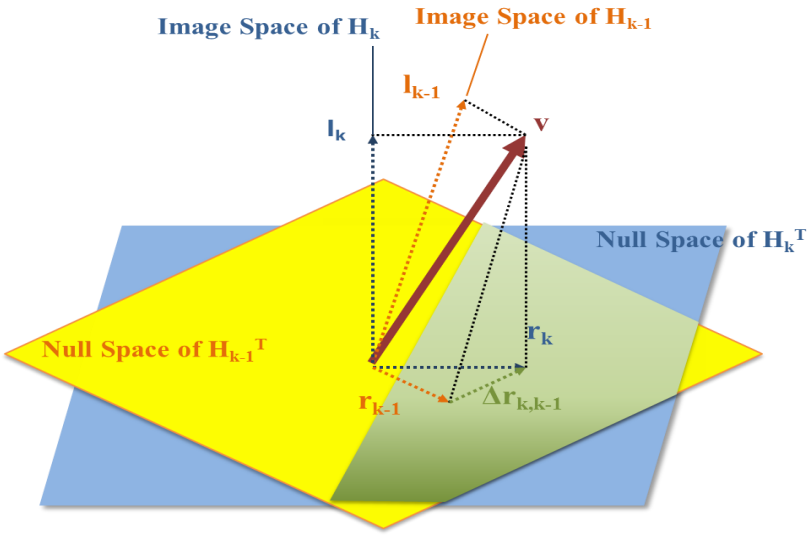

Fig. 3. Composition of the error vector

Assuming that the bias component of the error vectors in the current epoch is the same as those of the past two epochs, i.e. $\mathbf{v}_k \cong \mathbf{v}_{k-1} \cong \mathbf{v}_{k-2} = \mathbf{v}$, a new formulation is derived from Eq. (3):

$$\begin{aligned} \mathbf{r}_k + \mathbf{H}_k\mathbf{K}_k\mathbf{v} &= \mathbf{r}_{k-1} + \mathbf{H}_{k-1}\mathbf{K}_{k-1}\mathbf{v} \\ \mathbf{r}_k + \mathbf{H}_k\mathbf{K}_k\mathbf{v} &= \mathbf{r}_{k-2} + \mathbf{H}_{k-2}\mathbf{K}_{k-2}\mathbf{v} \end{aligned} \tag{9}$$

$$\begin{bmatrix} \mathbf{r}_k - \mathbf{r}_{k-1} \\ \mathbf{r}_k - \mathbf{r}_{k-2} \end{bmatrix} = \begin{bmatrix} -\mathbf{H}_k & \mathbf{H}_{k-1} & \mathbf{O} \\ -\mathbf{H}_k & \mathbf{O} & \mathbf{H}_{k-2} \end{bmatrix} \begin{bmatrix} \mathbf{K}_k\mathbf{v} \\ \mathbf{K}_{k-1}\mathbf{v} \\ \mathbf{K}_{k-2}\mathbf{v} \end{bmatrix} \tag{10}$$

Eq. (10) can be simplified as Eq. (11).

$$\Delta\bar{\mathbf{r}} = \mathbf{C}\cdot\mathbf{a} \tag{11}$$

where $\Delta\bar{\mathbf{r}} \triangleq \begin{bmatrix} \mathbf{r}_k - \mathbf{r}_{k-1} \\ \mathbf{r}_k - \mathbf{r}_{k-2} \end{bmatrix}$, $\mathbf{C} \triangleq \begin{bmatrix} -\mathbf{H}_k & \mathbf{H}_{k-1} & \mathbf{O} \\ -\mathbf{H}_\mathbf{k} & \mathbf{O} & \mathbf{H}_{k-2} \end{bmatrix}$ and $\mathbf{a} \triangleq \begin{bmatrix} \mathbf{K}_k\mathbf{v} \\ \mathbf{K}_{k-1}\mathbf{v} \\ \mathbf{K}_{k-2}\mathbf{v} \end{bmatrix}$.

The unknown vector $\mathbf{l}_k$, the lost component of $\mathbf{v}_k$, can be estimated utilizing the differences between the observation matrix and projections on it, as per Eq. (12). Finally, the error vector can be reconstructed using Eqs. (8) and (13). This algorithm uses measurements of the current and past two epochs. Thus, it can estimate the error vector without latency.

$$\hat{\mathbf{a}} = \left[\left(\mathbf{C}^T\mathbf{C}\right)^{-1}\mathbf{C}^T\right]\cdot\Delta\bar{\mathbf{r}} \tag{12}$$

$$\hat{\mathbf{l}}_k = \mathbf{H}_k\cdot\hat{\mathbf{a}}_k \tag{13-1}$$

$$\hat{\mathbf{v}}_k = \mathbf{r}_k + \hat{\mathbf{l}}_k \tag{13-2}$$

where $\hat{\mathbf{a}}_k$ consists of the first four components of $\hat{\mathbf{a}}$.

To solve Eq. (12), two important problems must be considered. The first problem is the ill conditioning of the system matrix, due to the considerable distance between the user's receiver and the satellites. Under this condition, the matrices $\mathbf{H}_k$, $\mathbf{H}_{k-1}$, and $\mathbf{H}_{k-2}$ contain similar components, and the system matrix $\mathbf{C}$ becomes difficult to invert. An ill-conditioned system makes the algorithm sensitive to variations in the error vector $\mathbf{v}$. As previously mentioned, the magnitude of the error vector $\mathbf{v}$ can be considered as the sum of the bias component and noise component of the range measurements. If the bias components in the (k-2) to k-th epochs are assumed to be constant vectors, only the noise components affect the error vector estimation. The ill-conditioned system significantly amplifies the noise level of the range measurements during the system matrix inversion. The resultant high noise level can yield a wrong estimation of the error vector. If the range measurements are acquired more precisely, the solution will be more robust, and its noise level in error vector estimation will be reduced. A lower measurement noise contributes to a smaller value of MDB as well as greater robustness of the

algorithm. The next section describes the new formulation of the algorithm adopting the RRAIM concept for lower range measurement noise levels.

Another problem is the linear dependency of the system. Similarly to the 2D case, in order to estimate a valid $\mathbf{l}_k$, the subspace of every epoch in Fig. 3 should be linearly independent, i.e. the null spaces at epoch k and epoch k-1 should be independent. The same fact applies to the image spaces. However, the image space of each observation matrix shares the same subspace, which spans column $\begin{bmatrix}-1 & -1 & \cdots & -1\end{bmatrix}^T$. Due to this column, the image spaces and null spaces of each observation matrix do not satisfy the property of linear independency between epochs. The column $\begin{bmatrix}-1 & -1 & \cdots & -1\end{bmatrix}^T$ is involved in calculating receiver clock error and does not affect the position solution. Therefore, this common component is not critical for integrity monitoring, and the receiver clock error is estimated independently from the main FDE process and assumed to be a common component. Due to the ill-conditioned system problem, both a precise receiver clock estimation and precise range measurements are required. For a precise receiver clock estimation, the kinematic Kalman filter is used with pseudorange and time difference carrier phase measurements (Kim, 2005). The receiver clock errors can thus be estimated accurately to within several millimeters. The proposed algorithm regards the receiver clock error as a common component and calculates lost components without taking into account the effects of common components. In this case, Eqs. (3) and (4) can be rewritten as the following equations:

$$\mathbf{r}_k' = \mathbf{z}_k - \mathbf{H}\hat{\mathbf{x}}_k' \tag{14-1}$$

$$\mathbf{P}_k' \triangleq \mathbf{H}_{k,1:3} \cdot \mathbf{K}_k' \triangleq \mathbf{H}_{k,1:3} \cdot \left[\mathbf{H}_{k,1:3}{}^T \mathbf{R}_k{}^{-1} \mathbf{H}_{k,1:3}\right]^{-1} \mathbf{H}_{k,1:3}{}^T \mathbf{R}_k{}^{-1} \tag{14-2}$$

where $\hat{\mathbf{x}}_k'$ is composed of a 3×1 user position estimation vector and 1 receiver clock estimation, which is calculated from the independent clock estimation filter. $\mathbf{H}_{k,1:3}$ is an $N\times3$ observation matrix, which consists of the first three columns of $\mathbf{H}_k$.

The proposed algorithm has a weakness. It is derived from the assumption that the bias component of error vector **v** is constant for the k-2 to k epochs. Therefore, if the magnitude of error exceeding a certain level varies with time, all the estimations at each line of sight will have very large values. As a result, although the algorithm detects occurrences of drifting error, it cannot identify which measurement has the error. For the same reason, if a constant bias occurs, a fault

identification is delayed for 2 seconds while the fault is detected without latency. This identification delay problem is not critical because it still meets the TTA requirement of 6 seconds.

4 RRAIM-adopting algorithm formulation

As mentioned in the previous section, in order to obtain a reliable estimation of error vector, precise range measurement is required to minimize the effect of the ill-conditioned system matrix. The most common way of getting precise GNSS ranging measurements is to use the carrier phase measurement as a ranging source. The carrier phase measurement has a much lower noise level than a pseudo-range measurement would. Therefore, it is applied in the fields that require high positioning accuracy, such as surveying and Precise Point Positioning (PPP). However, as the measured carrier phase contains a constant unknown integer ambiguity, it cannot be directly used as a ranging source. Resolving the carrier phase integer ambiguity is another challenging problem. In order to do this, the user must be heavily dependent on data from the ground facility. Because the data transfer rate of the ground facility is limited, heavy dependency on the ground channel can cause a failure to meet TTA requirements. In order to make the best use of precise carrier phase measurements without resolving integer ambiguity, the proposed algorithm adopts the RRAIM concept.

In the RRAIM concept, the receiver uses carrier-smoothed pseudo-range measurements, which are validated by the GIC, and propagates these measurements forward in time by compensating for the difference between current and past carrier phase measurements.

$$\hat{\rho}_k = \rho_{k-M} + \Delta\phi_{k,k-M} \tag{15}$$

where $\hat{\rho}_k$ is measured at the current epoch, k, propagated from the past GIC-corrected, ionosphere-free, and carrier-smoothed pseudo-range at 'k-M' (ρ_{k-M}), and $\Delta\phi_{k,k-M}$ is the difference in carrier phase measurements between epochs k and k-M. The propagated range measurement can be related to the true range, r, between the user and the satellite, as Eq. (16) shows:

$$\hat{\rho}_k = r_k + \tau_k + \delta\rho_{k-M} + \delta\Delta\phi_{k,k-M} \tag{16}$$

where τ is the receiver clock bias, $\delta\rho_{k-M}$ is the error in ρ_{k-M}, and $\delta\Delta\phi_{k,k-M}$ is the error in $\Delta\phi_{k,k-M}$. $\delta\rho_{k-M}$ is defined as normally distributed with the variance specified by Eq. (17).

$$\sigma_{\rho,j}^2 = \sigma_{clk\_eph,j}^2 + \sigma_{DF\_air,j}^2 + \sigma_{tropo,j}^2 \tag{17}$$

$\sigma_{\rho,j}^2$ means a variance of the j-th line of sight for $\delta\rho_{k-M}$. The error in ρ_{k-M} (i.e. $\delta\rho_{k-M}$) is assumed to be a sum of three independent error components. $\sigma_{clk\_eph,j}^2$ is the variance of residual error in the GIC-generated range correction (accounting for satellite clock and orbit errors), $\sigma_{DF\_air,j}^2$ is variance of carrier-smoothed code receiver noise and multipath, and $\sigma_{tropo,j}^2$ is the variance of residual tropospheric error. The error term $\delta\Delta\phi_{k,k-M}$ in Eq. (15) is also the sum of three independent error components; the change in carrier phase receiver noise and multipath over time interval M, the change in tropospheric error over the time interval, and the satellite clock drift over the time interval. These errors are also modeled as a zero mean normal distribution with standard deviations of $\sigma_{\Delta(n+mp)}$, $\sigma_{\Delta trop}$, and $\sigma_{\Delta clk}$.

$$\sigma_{\Delta\phi,j}^2 = \sigma_{\Delta(n+mp),j}^2 + \sigma_{\Delta trop,j}^2 + \sigma_{\Delta clk,j}^2 \tag{18}$$

The methods for specifying each standard deviation in Eq. (16) and (17) are well described in (GEAS, 2008). The error covariance matrix associated with $\delta\rho_{k-M}$ for N satellites in view is $\mathbf{R}_{\delta\rho} = diag\left(\sigma_{\rho,1}^2,\cdots,\sigma_{\rho,N}^2\right)$, and with $\delta\Delta\phi_{k,k-M}$ it is $\mathbf{R}_{\delta\Delta\phi} = diag\left(\sigma_{\Delta\phi,1}^2,\cdots,\sigma_{\Delta\phi,N}^2\right)$. The total error associated with the propagated ranging measurements, $\hat{\rho}_k$, in Eq. (14) for N satellites is then described by the covariance matrix $\mathbf{R}_{\delta\hat{\rho}} = \mathbf{R}_{\delta\rho} + \mathbf{R}_{\delta\Delta\phi}$.

The RRAIM measurement and covariance matrix discussed in this section can be related to equations in the previous section. The observation in Eq. (1) can be rewritten so that it adopts the RRAIM measurement model, becoming Eq. (19).

$$\begin{bmatrix} \hat{\rho}_{k,1} \\ \vdots \\ \hat{\rho}_{k,N} \end{bmatrix} = \mathbf{H} \begin{bmatrix} \mathbf{x}_k \\ \tau_k \end{bmatrix} + \begin{bmatrix} \delta\hat{\rho}_{k,1} \\ \vdots \\ \delta\hat{\rho}_{k,N} \end{bmatrix} + \boldsymbol{\beta} \tag{19}$$

The range measurement $\mathbf{z}$ is a carrier-propagated code measurement that is validated from the GIC, and the error vector $\mathbf{v}$ is expressed as a sum of the noise component $\delta\hat{\rho}_k$ and unknown bias component $\boldsymbol{\beta}$. In this case, $\mathbf{R}_k$ in Eq. (3) is $\mathbf{R}_{\delta\hat{\rho}}$, and the RRAIM-adopted FDE equations can be rearranged by associating the RRAIM measurement and its covariance matrix with Eqs. (7) - (13). The measurement noise can be easily reduced by adopting the RRAIM concept. However, when updating the pseudo-range measurement at the end of the coasting time, the pseudo-range noise causes a problem in the FDE process. Because the noise level of pseudo-range measurement is very large compared with that of carrier phase measurement, noise in a new pseudo-range measurement has an effect similar to a range bias for the extent of the coasting time. In other words, if the pseudo-range is updated at the k-th epoch, then nominal bias due to the pseudo-range noise in $\hat{\rho}_k$ becomes different from that of $\hat{\rho}_{k-1}$ and $\hat{\rho}_{k-2}$. This nominal bias change occurs in every pseudo-range update at the end of each coasting time interval. Furthermore, this nominal bias change breaks the assumption that the error vector is constant for 3 consecutive epochs. Therefore, the FDE algorithm raises a false alarm during the 2 epochs after every pseudo-range update. From the (k+2)-th epoch to the next pseudo-range update, $\hat{\rho}_k$, $\hat{\rho}_{k+1}$, $\cdots$, $\hat{\rho}_{k+M}$ have the same nominal bias, causing a false alarm due to the fact that no change occurs in pseudo-range noise. With only a single set of test statistics, continuous FDE cannot be conducted because of the false alarms. This problem can be resolved using 2 test statistics in parallel. Fig. 4 shows the concept of the parallel test statistics.

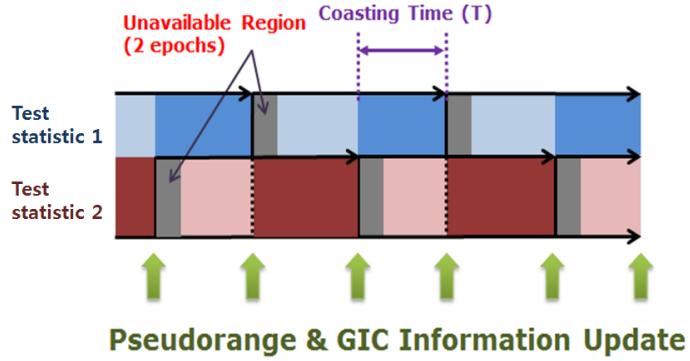

Fig. 4. Parallel test statistics

Here, GIC information and pseudo-range are updated every T seconds, and the test statistics are unavailable for every second from T to T+1 (gray region). One measurement updates the pseudo-range and GIC information at 1T, 3T, ⋯ , (2n-1)T seconds, and the other one updates the information at 2T, 4T, ⋯, (2n)T seconds (where n is a positive integer). Via this procedure, at least one test statistic is available during every coasting time (dark blue and dark red regions).

5 Simulation results

Simulations are conducted to verify the feasibility of the proposed algorithm. The satellite orbit is generated using the RINEX navigation files. In this simulation, it is assumed that the GIC provides users with correction messages and integrity messages every 30 seconds. The user can obtain integrity-assured measurements by applying the information from the GIC. It is also assumed that ionospheric delay, tropospheric delay, satellite orbit and clock errors are eliminated with the help of the GIC information. Under these assumptions, for each line of sight, a random noise with a standard deviation modeled as a function of satellite elevation angle is added to each geometrical range. In addition to this, various combinations of biases are inserted at t = 50 to 100 seconds.

Fig. 5 shows the results of the proposed algorithm using only pseudo-range measurements in a single failure case.

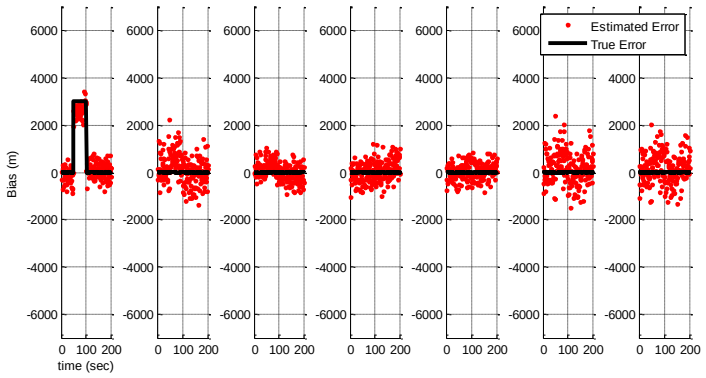

Fig. 5. Results of the algorithm when using only pseudorange measurements

The proposed algorithm can detect failures with a magnitude on the order of several km because it is very sensitive to measurement noise due to the ill-conditioned system. Fig. 6 (a) and (b) are the results of the proposed algorithm and conventional WLS RAIM algorithm under a single failure condition with the following bias inserted:

bias = $[0\ 0\ 0\ 0\ 0\ 0\ 15]^{T}$ m

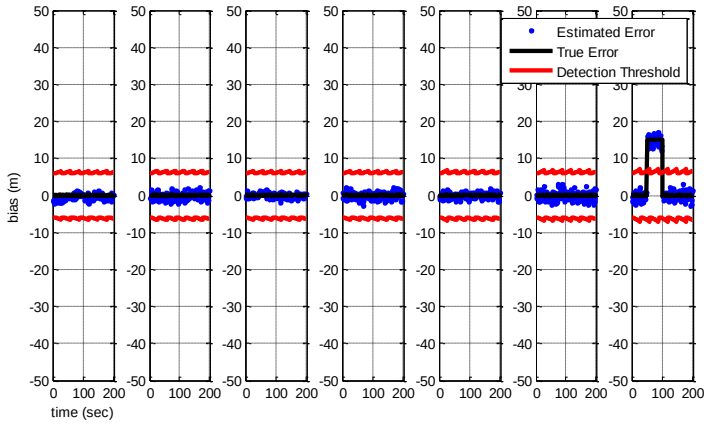

(a) Proposed algorithm

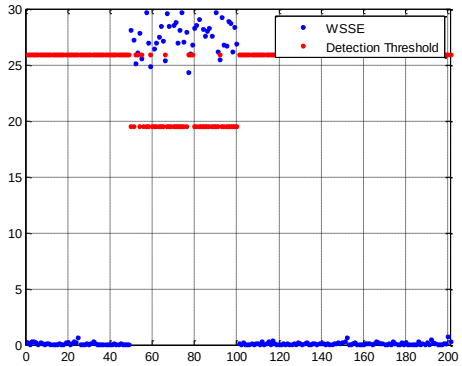

(b) Conventional WLS algorithm

Fig. 6. Results in case of bias = [0 0 0 0 0 0 15]T m

A comparison of Fig. 5 and Fig. 6 (a) indicates that the magnitude of detectable bias decreases considerably when the RRAIM concept is adopted for the range measurement. The carrier phase measurement and pseudo-range measurement result in MDBs of practical magnitudes. The proposed algorithm detects and identifies failures by directly estimating the individual components of errors and then determining whether the error is from the individual probability density function. The proposed algorithm yields a smaller value of MDB, and its identifying process is much simpler.

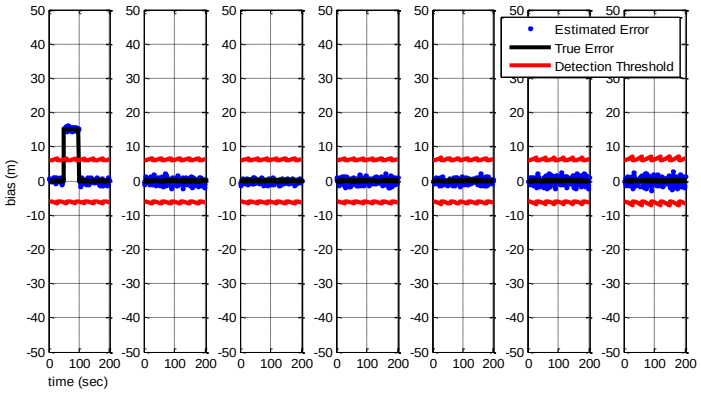

(a) Proposed algorithm

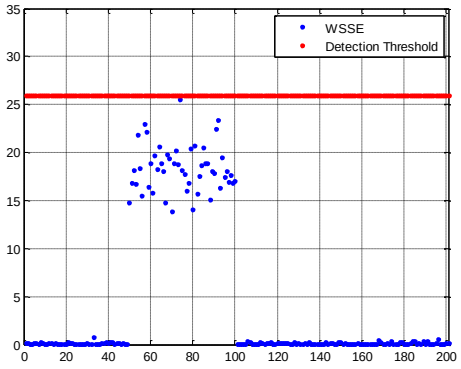

(b) Conventional WLS algorithm

Fig. 7. Results in case of bias = [15 0 0 0 0 0 0]T m

Fig. 7 shows the results of a different case of single failure. In this case, the magnitude of the error vector is the same as in the case depicted in Fig. 6, but the direction of the error vector is similar to the direction of the image space of the **H** matrix. Although the magnitude of bias is the same as in Fig. 6, the WLS algorithm cannot detect a failure at all. In this case, the impact of the bias on the test statistic is negligible, and the detection capability of the WLS algorithm is insufficient to protect the user even in the case of a single failure. Detection capability of the WLS algorithm depends on the direction of the error vector and satellite geometry. However, because the proposed algorithm utilizes not only a range residual vector but also a lost component, its detection capability is not dependent on satellite geometry. It is observed that analogous results are also valid in cases involving multiple failures.

Figs. 8 (a) and (b) are the results of each algorithm in a case involving multiple failures. In this simulation, in order to contrastively show the detection capability of each algorithm, the error vector is placed close to the image space of the **H** matrix, so that its projection on the null space (i.e. residual vector) is near zero. The following bias is inserted:

bias = $[0\ 0\ 0\ 0\ 15\ 0\ 15]^T$ m

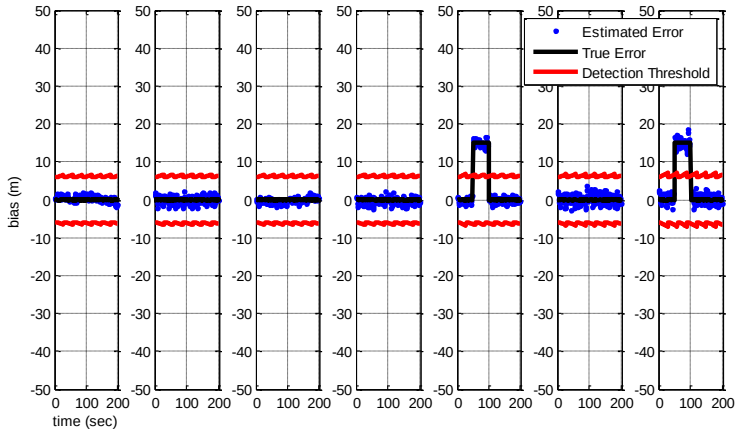

(a) Proposed algorithm

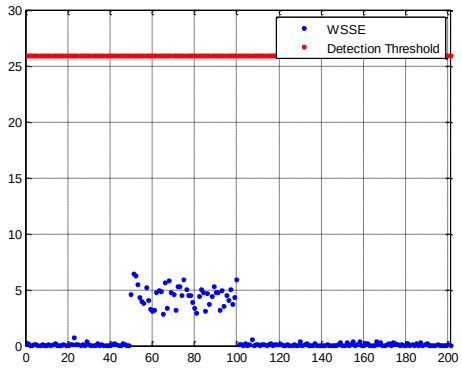

(b) Conventional WLS algorithm

Fig. 8. Results in case of bias = [0 0 0 0 15 0 15]T m

In this case, even if two failures of the same magnitude of bias occur, the test statistics of WLS have smaller values than they do in the single failure cases. The error vector is placed in the image space of the H matrix, resulting in the loss of most of it. Only a very small part remains available on the projected component. Therefore, the WLS algorithm is incapable of detecting any failure at all. As a

consequence, the position error will accumulate without any alarm. On the other hand, the proposed algorithm estimates the error vector accurately and successfully detects all faulty measurements.

6 Conclusions

The RAIM plays a key role in protecting the user against various failure conditions. However, the conventional WLS RAIM algorithm can protect only against single failures. In addition, because of a reduction in the threshold for failure detection, the probability of failure as redefined with improved accuracy may be higher than the probability of failure under the current requirements. Furthermore, an increased number of ranging sources makes it necessary to consider the possibility of simultaneous multiple failures. This paper presented a new multiple-hypothesis RAIM algorithm, which detects failures by monitoring the error vector itself instead of monitoring the projection of the error. The algorithm is able to detect any instance of multiple failures, including failures which are not detected by the conventional WLS algorithm. The algorithm estimates range errors using precise carrier phase measurements. Therefore, it is able to detect multiple failures with magnitudes of several tens of meters, although the algorithm has to solve the ill-conditioning problem. Simulation results show that the detection capability of the proposed algorithm is not dependent on satellite geometry. Therefore, even if the satellite geometry gets worse, the user's protection level will not increase too much. The MDB value, which is smaller than in previous works, makes it possible to use the algorithm in many practical applications.

6 Acknowledgements

This research was supported by a grant from "Development of Wide Area Differential GNSS," which is funded by Ministry of Land, Transport and Maritime Affairs of Korean government, contracted through SNU-IAMD at Seoul National University.

7 References

I. Martini, R. Wolf, and G. W. Hein, "Receiver Integrity Monitoring in Case of Multiple Failures," presented at the ION GNSS 19th International Technical Meeting, Fort Worth, TX, Sep., 2006.

T. Walter, and P. Enge, "Weighted RAIM for Precision Approach," presented at the ION 1995, Palm Springs, CA, 12-15 Sep., 1995.

C. Macabiau, B. Gerfault, I. Nikiforov, L. Fillatre, B. Roturier, E. Chatre, M. Raimondi and A. Esche, "RAIM Performance in Presence of Multiple Range Failures," presented at NTM 2005, San Diego, CA, 24-25, Jan, 2005.

A. Ene, J. Blanch, and J. D. Powell, "Fault Detection and Elimination for Galileo-GPS Vertical Guidance," presented at the ION NTM, San Diego, CA, 2007

J. Blanch, A. Ene, T. Walter, and P. Enge, "An Optimized Multiple Hypothesis RAIM Algorithm for Vertical Guidance," presented at the ION GNSS 20th International Technical Meeting of the Satellite Division, Fort Worth, TX, 25-28, Sep., 2007.

B. Pervan, S. Pullen, and J. Christie, "A Multiple Hypothesis Approach to Satellite Navigation Integrity," Navigation, vol. 45, no. 1, 1998.

J. Angus, "RAIM with Multiple Faults," Navigation, vol. 53, no. 4, 2006.

GNSS Evolutionary Architecture Study, Phase I – Panel Report, Feb., 2008, http://www.faa.gov/about/office_org/headquarters_offices/ato/service_units/techops/navservices/gnss/library/documents/media/GEAS_PhaseI_report_FINAL_15Feb08.pdf

V. Graas, A. Soloviev, "Coasting with relative carrier phase RAIM," in Briefing to GEAS Panel, Palo Alto, CA, Feb. 21-22, 2007.

L. Gratton, M. Joerger, and B. Pervan, "Carrier Phase Relative RAIM Algorithms and Protection Level Derivation," Journal of Navigation, Vol. 63, no. 2, April 2010.

Y. C. Lee and M. P. McLaughlin, " Feasibility Analysis of RAIM to Provide LPV 200 Approaches with Future GPS," presented at ION GNSS 2007, Fort Worth, TX. Sep., 2007.

J. H. Kim, "A Study on GPS-RTK Corrections suitable for Low-rate Data-link", ph. D. thesis, Seoul National University, Feb. 2005